SCIENTIFIC REP✹RTS

OPEN

Origin of sample size effect: Stochastic dislocation formation in crystalline metals at small scales

Guan-Rong Huang[1,2], J. C. Huang[1] & W. Y. Tsai[1]

In crystalline metals at small scales, the dislocation density will be increased by stochastic events of dislocation network, leading to a universal power law for various material structures. In this work, we develop a model obeyed by a probability distribution of dislocation density to describe the dislocation formation in terms of a chain reaction. The leading order terms of steady-state of probability distribution gives physical and quantitative insight to the scaling exponent n values in the power law of sample size effect. This approach is found to be consistent with experimental n values in a wide range.

Experiments have shown that crystalline metallic materials can be strengthened by sample size reduction[1,2], and this is so-called sample size effect governed by the empirical power law of scaling type, $s = d^{-n}$, where s is the scaling stress, d is the characteristic length scale of the sample, and n is the scaling exponent. With the progress in experiments at small scales, researchers can make a fine measurement on the mechanical properties of metals. For the past decades, researchers have found that the range of n is about 0.6 to 0.7 for face-centered cubic (FCC) metals while 0.3 to 0.8 for body-centered cubic (BCC) metals[3–11]. Recent studies also suggest that n lies within 0.3 to 1.0[12]. The general trend held for micro- to mini-scale seems to have nothing to do with crystal structure and sample geometry[2,13–16], which represents there should be a universal mechanism underlying in different metals.

The size effect of metals can be explained by using statistical techniques[17–19], namely, the stress or strain occurrs in stochastic events with some underlying probability distributions. The relation between stress and dislocation density is the double power law form during the process of dislocation source activation and/or dislocation forest hardening for different sample sizes and initial dislocation density[20,21]. Therefore, the mechanism of size effect is dependent on the dislocation density. Before applying stress, crystalline metals with a high degree of perfection at small scales possess a relatively lower order of dislocation density (about $10^4\,cm^{-2}$). Over extensive studies, it has been widely acknowledged that slip events occurred in crystals are conducted with the aid of dislocations. The plastic deformation in crystals corresponds to a large amount of dislocation formations, dislocation interactions and recoveries, which are generally regarded to be initiated from the Frank-Read or similar sources.

Experimental evidence shows that the Frank-Read or similar sources can act as the dislocation nucleation sites. For the sake of simplicity, homogeneous and heterogeneous dislocation nucleation are both merged as parts of dislocation nucleation, and they may generate a dislocation or recover to their original state. Additionally, experiments show that dislocation nucleation is driven by stress and diffusion-controlled process[12,22,23]. After dislocation nucleation, mobile dislocations can move and increase their length to accomplish the shape changes in metallic crystals, and hence the dislocation density will be increased. This increases the possibility of dislocation interactions leading to dislocation recovery. Thus, Fig. 1 exhibits the universal mechanism for dislocation formation in different metals to describe the dynamics of dislocation density and to relate the physical meaning of scaling exponent n in sample size effect to experimental observations. In Fig. 1, k_1 is the dislocation nucleation rate of nucleation site into dislocation nucleation driven by stress, k_2 is the rate of dislocation formation after nucleation into dislocation multiplication, where mobile dislocations can glide and increase their length, γ_1 is the recovery rate of dislocation nucleation, γ_2 is the recovery rate of dislocation, and D is the dislocation nucleation rate of nucleation site into dislocation nucleation driven by diffusion process. Then it will be considered in later section that the overall generation of dislocation is characterized by two parameters: the effective mean number of dislocation nucleation during the life time of dislocation, $\alpha = (k_1 + D)/\gamma_2$, and the mean number of dislocation multiplication during the life time of dislocation nucleation, $\beta = k_2/\gamma_1$. The life time of nucleation is assumed to be

[1]Department of Materials and Optoelectronic Science, National Sun Yat-Sen University, Kaohsiung 804, Taiwan, ROC. [2]Physics Division, National Center for Theoretical Sciences, Hsinchu 30013, Taiwan, ROC. Correspondence and requests for materials should be addressed to G.-R.H. (email: d01222004@ntu.edu.tw)
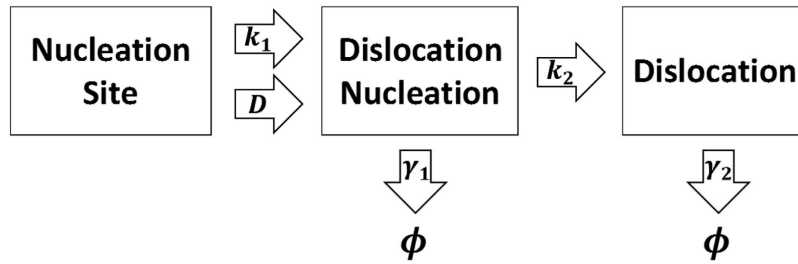
Figure 1. The mechanism of dislocation formation driven by the plastic events plus thermally-activated diffusion process on single crystal metals at small scales.

short compared to that of dislocation, where the plastic events can be counted as the uncorrelated random events. In a word, dislocations are created by the plastic deformation plus thermally-activated diffusion.

Since these events increasing the dislocation density are all stochastic processes, the stochastic differential equation of PD in terms of dislocation density and time can describe the dynamics of dislocation density. With the known dynamics of PD, the dynamics of stress can be established through the relation between dislocation density and stress. With the known PD in Eq. (7), the trajectory of plastic deformation can be counted as a sequence of steady-state dislocation density, which gives the n value via the algorithm in refs 17,18 and exponent τ value in ref. 19.

Dislocation Stochastic Formation and Scaling Exponent

To investigate the dynamics of dislocation network, we can introduce a master equation, the equation of motion for PD. In ref. 24, the simple mechanism in Fig. 1 with a fluctuation term can be described by the stochastic differential equation in terms of dislocation density ρ and time t

$$d\rho = b(\rho)dt + d\Gamma_t + \sqrt{2a}\,dB_t, \tag{1}$$

where $b(\rho)$ is the deterministic term, Γ_t is the stochastic process driven by plastic deformation, and B_t is the fluctuation term. Γ_t is compound noise with impulsive Poisson distribution, and B_t is Gaussian noise and fluctuation around a global extrema. Both they are stochastic processes with independent increment. Equation (1) is size-dependent[25,26], since the mechanism of dislocation source activation and dislocation forest hardening depends on the initial dislocation density and sample size. Common deformation tests are conducted at nearly constant temperature, the temperature effect on reaction rates can be neglected during tests. The corresponding master equation of Eq. (1) for the PD $P(\rho, t)$ is expressed as

$$\frac{\partial P(\rho, t)}{\partial t} = a\frac{\partial^2 P(\rho, t)}{\partial \rho^2} - \frac{\partial}{\partial \rho}[b(\rho)P(\rho, t)]$$
$$+ k_1\left[\int_0^\rho P(\rho - \rho', t)w(\rho')d\rho' - P(\rho, t)\right], \tag{2}$$

where the a value corresponding to B_t is the magnitude of fluctuation, the integration term corresponding to Γ_t can be counted as the reaction of dislocation formation induced by plastic deformation, and $w(\rho')$ is the average transition probability density from dislocation nucleation into dislocation in the material. In the integration term of Eq. (2), $P(\rho - \rho', t)w(\rho')d\rho'$ is the transition probability from $\rho - \rho'$ to ρ. Hence, it is reasonable to assume $w(\rho')$ as the exponential decay function, $\frac{1}{\beta}e^{-\frac{\rho'}{\beta}}$. On the other hand, the annihilation rate of dislocation increases with increasing dislocation density due to the attraction among opposite signed dislocations and the reduction of overall dislocation strain energy[27,28]. Thus, the recovery term is set as $b(\rho) = -\gamma_2\rho$. Therefore, Eq. (2) with such $b(\rho)$ and $w(\rho')$ is re-written as

$$\frac{\partial P(\rho, t)}{\partial t} = a\frac{\partial^2 P(\rho, t)}{\partial \rho^2} + \gamma_2\frac{\partial}{\partial \rho}[\rho P(\rho, t)]$$
$$+ \frac{k_1}{\beta}\left[\int_0^\rho P(\rho - \rho', t)e^{-\frac{\rho'}{\beta}}d\rho' - \beta P(\rho, t)\right], \tag{3}$$

and the corresponding mean of dislocation density with time evolution is

$$\overline{\rho}(t) = \int_0^\infty \rho P(\rho, t)d\rho. \tag{4}$$

For the steady-state of Eq. (3), $\frac{\partial P(\rho, t)}{\partial t} = 0$, the solution solved in ref. 29 is expressed as the combination of the Kummer's functions. In ref. 20, flow stress is connected to dislocation density in double power law form

$$s = \frac{c_1}{\rho^{\mu}} + c_2\rho^{\mu},$$

(5)

where c_1 is inverse proportional to sample size, c_2 is a constant, and $\mu = \frac{1}{2}$. There exists a critical dislocation density as a function of sample size, $\rho_c = c_1/c_2$, where it is the transition between dislocation source activation and dislocation forest hardening[20,30–32]. Below ρ_c the mechanism of dislocation source activation will gradually become dominant with decreasing dislocation density. Likewise, above ρ_c the mechanism of dislocation forest hardening or dislocation multiplication will gradually become dominant with increasing dislocation density. For ρ away from ρ_c, the relation of s and ρ is simple power law form, and thus $P(s) = P\left(\rho = \left(\frac{c_1}{s}\right)^{\frac{1}{\mu}}\right)\left|\frac{d\rho}{ds}\right|$ for $\rho \ll \rho_c$ or $P\left(\rho = \left(\frac{s}{c_2}\right)^{\frac{1}{\mu}}\right)\frac{d\rho}{ds}$ for $\rho \gg \rho_c$. In general cases, the a value is much smaller than the γ_2 value, and thus the a term of Eq. (2) can be neglected without loss of generality. Therefore, $P(\rho)$ without the a term of Eq. (3) solved in ref. 33 is

$$P(\rho) = \frac{1}{\beta\Gamma(\alpha)}\left(\frac{\rho}{\beta}\right)^{\alpha-1} e^{-\rho/\beta},$$

(6)

and the corresponding PD in terms of s is

$$P(s) = \begin{cases} \dfrac{A}{c_1}\left(\dfrac{c_1}{s}\right)^{\frac{\alpha}{\mu}+1} \exp\left[-\left(\dfrac{c_1}{\beta^{\mu}s}\right)^{\frac{1}{\mu}}\right], & \rho \ll \rho_c \\[4mm] \dfrac{A}{c_2}\left(\dfrac{s}{c_2}\right)^{\frac{\alpha}{\mu}-1} \exp\left[-\left(\dfrac{s}{\beta^{\mu}c_2}\right)^{\frac{1}{\mu}}\right], & \rho \gg \rho_c \end{cases},$$

(7)

where $A = [\mu\beta^{\alpha}\Gamma(\alpha)]^{-1}$. The second line in Eq. (7) is the form of generalized gamma distribution which has been used in statistical simulation for stress dynamics in refs 17,18. Finally, the dislocation density of steady-state ρ_s is

$$\rho_s = \int_0^{\infty} \rho P(\rho)d\rho = \beta\frac{\Gamma(\alpha+1)}{\Gamma(\alpha)} = \alpha\beta.$$

(8)

For common deformation tests, the strain rate is a small value in the $10^{-4}s^{-1} \sim 10^{-5}s^{-1}$ order. The strain rate is so slow that the deformation process can be counted as a series of steady state processes corresponding to different β values. Therefore, the deformation process can be characterized as a series of β values or ρ_s values like the sequence: $\{\beta_1, \beta_2, \ldots\}$ or $\{\rho_{s_1}, \rho_{s_2}, \ldots\}$, where the different β and ρ_s values correspond to different steady-state processes.

With the aid of refs 17–19,34, the scaling exponent n can be constructed through $P(s)$

$$n = \begin{cases} 1 - \mu(\tau+1)/\alpha = n_1, & \rho \ll \rho_c \\ \mu(\tau+1)/\alpha = n_2, & \rho \gg \rho_c \end{cases},$$

(9)

where τ is the exponent in the envelope distribution for the normalized strain in refs 19,35. The α values in the two lines of Eq. (9) are different since they correspond to different mechanisms, dislocation source activation and dislocation forest hardening. For the intermediate region, $\rho < \rho_c$ or $\rho > \rho_c$, the asymptotic relation of s and ρ can be obtained by binomial expansion

$$\rho \approx \begin{cases} [(s/c_1)^{\frac{1}{\mu}} - 2(c_2/c_1)]^{-1}, & \rho < \rho_c \\ (s/c_2)^{\frac{1}{\mu}} - 2c_1/c_2, & \rho > \rho_c \end{cases},$$

(10)

which gives the scaling exponent

$$n \approx \begin{cases} n_1 - (n_1+\mu-1)(1+c_3x^{1-\frac{1-n_1}{\mu}})^{-1}, & \rho < \rho_c \\ n_2 - (n_2-\mu)(1+c_4x^{\frac{n_2}{\mu}-1})^{-1}, & \rho > \rho_c \end{cases},$$

(11)

where c_3 and c_4 are both constants and $x = 1/d$.

Discussion

For crystalline metals at small scales, we consider the master equation of PD as a function of dislocation density, where dislocations are produced by the deformation of the material plus diffusion processes. In the material, the generation and annihilation of dislocations are characterized by the constants of reaction rate: k_{1-2} and γ_{1-2}. As time past, the mean of dislocation density governed by Eq. (4) will reach a critical value ρ_s in Eq. (8), where the

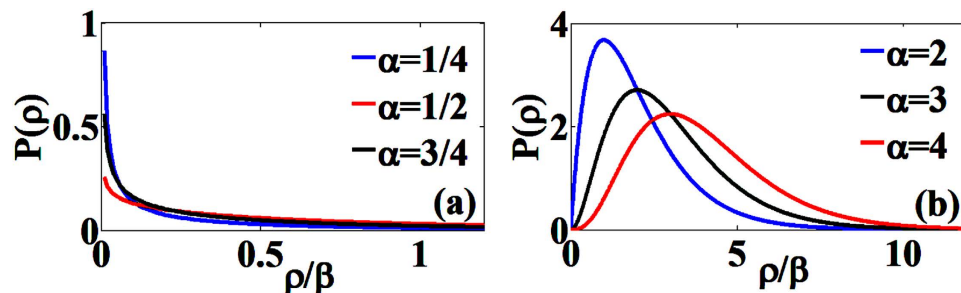**Figure 2.** (**a**) The steady-state PD predicted by Eq. (6) for $\alpha < 1$ with $\beta = 10$. (**b**) The steady-state PD predicted by Eq. (6) for $\alpha > 1$ with $\beta = 10$ and the unit of y-axis is 10^{-2}.
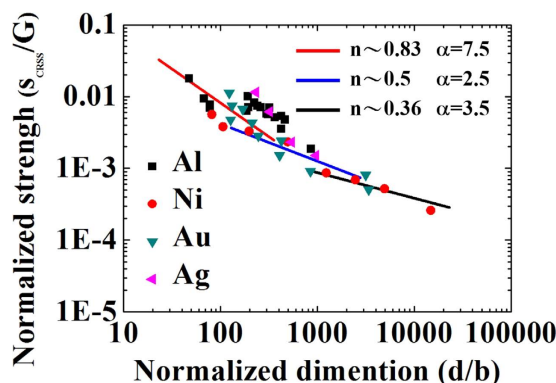

Figure 3. The comparison between experimental results and *n* values predicted in Eq. (9), where $\mu = \frac{1}{2}$ and $\tau = \frac{3}{2}$ are used. The data points were extracted from experiments in refs 1,2,8–10,16,37–39 with different single crystal metals listed.

plastic event occurs and the dislocation density of steady-state is characterized by the parameter, $\alpha\beta = (k_1 + D)k_2/\gamma_1\gamma_2$. It is considered as chemical equilibrium, where the ratio of forward reaction rate $(k_1 + D)k_2$ to backward reaction rate $\gamma_1\gamma_2$ is a constant. The double power law relation of *s* and ρ has been used to construct the PD in terms of stress *s*. The different stress and β values correspond to different steady-state dislocation density, and the deformation process can be counted as a sequence of dislocation density, $\{\rho_{s_1}, \rho_{s_2}, ...\}$.

For many crystalline metals at small scales, the τ is $\frac{3}{2}$, $D \ll \gamma_2$, and $\mu = \frac{1}{2}$ corresponding to $\alpha \approx k_1/\gamma_2 \approx \frac{5}{4(1-n)}$ or $\frac{5}{4n}$ and $n \approx 1 - \frac{5}{4\alpha}$ or $\frac{5}{4\alpha}$, depending on the dislocation density and sample size. The *n* value is only sightly altered by diffusion nucleation. In this study, α can vary from 0 to ∞, depending on the relative weighting of $k_1 + D$ versus γ_2. For example, if $\alpha = 0.25$, 0.5, 1.5, 2.5, 3.5, and 4.5, *n* would equal −4, −1.5, 0.17, 0.5, 0.64, and 0.72 for $\rho \ll \rho_c$ or 5, 2.5, 0.83, 0.5, 0.36, and 0.28 for $\rho \gg \rho_c$. According to experiments, the general cases are approximately in the regime of $0.75 \leq n \leq 0.85$ for $\rho \gg \rho_c$ or $0.3 \leq n \leq 0.4$ for $\rho \gg \rho_c$, resulting in $5 \leq \alpha \leq 8.3$ for $\rho \ll \rho_c$ or $3.1 \leq \alpha \leq 4.2$ for $\rho \gg \rho_c$. As stated before, α is defined as the effective mean number of dislocation nucleation, so the physical meaning of α can be related to the activation of dislocation sources or the average number of active slip systems. In the regime of initial dislocation density above ρ_c, the mechanism is mainly dislocation forest hardening or dislocation multiplication, and thus only dislocations nucleated right on these planes of active slip systems will be increased in length drastically, while dislocations nucleated on other planes may die out through dislocation recovery or keep in relatively small length since these dislocations can not glide to increase their length. Thus, the α value should be proportional to the average number of active slip systems. For metal crystals, the number of active slip systems is from 2 to 5 depending on the crystal structure, FCC or BCC. Therefore, the $\alpha < 1$ case would not be realistic, meaning that no slip system is well-activated. For a metal with more active slip systems, it has weaker size effect, and vice versa. Generally, BCC metals with less active slip systems would have higher *n* (lower α) value than FCC metals with more active slip systems would have. In ref. 36, the *n* value is related to initial dislocation density, samples with more dislocation density would have lower *n* value. Here, it means that a metal with more initial dislocation density would have higher α value. Since initial dislocations have occupied more sites which may be randomly distributed in space, some of these sites are on the planes of active slip systems. Thus, there exists more effective sites for dislocation nucleation (higher α), and vice versa. In the regime of initial dislocation density below ρ_c, the mechanism is mainly dislocation source activation which leads to dislocation source strengthening, and thus *n* will increase with increasing α. Low α values would not be taken as real cases, since the dislocation formation mainly comes from dislocation nucleation without dislocation multiplication. For the initial dislocation density in intermediate regime, $\rho \approx \rho_c$, there is a competi-

tion among source strengthening, forest hardening, and exhaustion hardening. It is hard to determine the accurate form of n due to the complex transitions among these mechanisms. Equation (11) gives the asymptotic behaviour of n in first order approximation, and it can be noted that n and ρ_c will both increase with decreasing d. It is the fact that dislocation source strengthening will gradually become dominant with decreasing d, and thus the n value will be increased. The mechanism governed by Eq. (3) is random and uncorrelated events, and it leads to the PD in terms of s for $\rho \gg \rho_c$, which is the same form of PD in refs 17,18, where their PD are generalized gamma distributions. For both $\rho \ll \rho_c$ and $\rho \gg \rho_c$ regimes, the leading order term of PDs are proportional to $s^{\pm\frac{\alpha}{\mu}-1}$. As shown in Fig. 2, the PD is characterized by the α value, and thus dislocation generation is strongly affected by the dislocation source activation and the average number of active slip systems. For $\alpha < 1$ cases corresponding to $n < -0.25$ for $\rho \ll \rho_c$ or $n > 1.25$ for $\rho \gg \rho_c$, the dislocation annihilation rate is larger than dislocation nucleation rate, and thus the maximum of distribution is located at $\rho = 0$. For $\alpha > 1$ cases corresponding to $n > -0.25$ for $\rho \ll \rho_c$ or $n < 1.25$ for $\rho \gg \rho_c$, the maximum of distribution is located at $\rho = \beta(\alpha - 1)$, where α is increased by dislocation source activation, or the active slip systems for dislocations are initiated with a high effective number of dislocation nucleations. Figure 3 shows the double-logarithm plot for normalized strength and normalized sample size extracted from refs 1,2,8–10,16,37–39, where the n and α have different values across different regimes: dislocation source activation ($n \sim 0.83$ and $\alpha \sim 7.5$), transition from dislocation source activation to dislocation forest hardening ($n = 0.5$ and $\alpha \sim 2.5$), and dislocation forest hardening ($n = 0.36$ and $\alpha \sim 3.5$). For the present of small a term, the maximum point and general shape of $P(\rho)$ does not change, and it only changes the $P(\rho)$ value at $\rho = 0$ to a finite value[29]. Thus, the general form of Eq. (6) will not change. Our analytic results straightforwardly provide a microscopic theory and mechanism in understanding the physical insight of α and the universal power law in sample size effect.

References

1. Uchic, M. D., Dimiduk, D. M., Florando, J. N. & Nix, W. D. Sample dimensions influence strength and crystal plasticity. *Science* **305,** 986–989 (2004).
2. Dimiduk, D. M., Uchic, M. D. & Parthasarathy, T. A. Size-affected single-slip behavior of pure nickel microcrystals. *Acta Mater.* **53,** 4065–4077 (2005).
3. Uchic, M. D., Shade, P. A. & Dimiduk, D. M. Plasticity of micrometer-scale single crystals in compression. *Annu. Rev. Mater. Res.* **39,** 361–386 (2009).
4. Kraft, O., Gruber, P. A., Mnig, R. & Weygand, D. Plasticity in confined dimensions. *Annu. Rev. Mater. Res.* **40,** 293–317 (2010).
5. Greer, J. R. & Hosson, J. T. M. D. Plasticity in small-sized metallic systems: Intrinsic versus extrinsic size effect. *Prog. Mater. Sci.* **56,** 654–724 (2011).
6. Dou, R. & Derby, B. A universal scaling law for the strength of metal micropillars and nanowires. *Scripta Mater.* **61,** 524–527 (2009).
7. Jennings, A. T., Burek, M. J. & Greer, J. R. Microstructure versus size: mechanical properties of electroplated single crystalline Cu nanopillars. *Phys. Rev. Lett.* **104,** 135503 (2010).
8. Greer, J. R. & Nix, W. D. Nanoscale gold pillars strengthened through dislocation starvation. *Phys. Rev. B* **73,** 245410 (2006).
9. Frick, C. P., Clark, B. G., Orso, S., Schneider, A. S. & Arzt, E. Size effect on strength and strain hardening of small-scale [111] nickel compression pillars. *Mater. Sci. Eng. A* **489,** 319–329 (2008).
10. Wang, Z.-J. *et al.* Sample size effects on the large strain bursts in submicron aluminum pillars. *Appl. Phys. Lett.* **100,** 071906 (2012).
11. Yu, Q. *et al.* Strong crystal size effect on deformation twinning. *Nature* **463,** 335–338 (2010).
12. Abbaschian, R., Abbaschian, L. & Reed-Hill, R. E. *Physical Metallurgy Principles* (Cengage Learning, 2010).
13. Greer, J. R., Oliver, W. C. & Nix, W. D. Size dependence of mechanical properties of gold at the micron scale in the absence of strain gradients. *Acta Mater.* **53,** 1821–1830 (2005).
14. Hodge, A. M. *et al.* Scaling equation for yield strength of nanoporous open-cell foams. *Acta Mater.* **55,** 1343–1349 (2007).
15. Ng, K. S. & Ngan, A. H. W. Stochastic nature of plasticity of aluminum micro-pillars. *Acta Mater.* **56,** 1712–1720 (2008).
16. Kunz, A., Pathak, S. & Greer, J. R. Size effects in Al nanopillars: Single crystalline vs. bicrystalline. *Acta Mater.* **59,** 4416–4424 (2011).
17. Derlet, P. M. & Maass, R. A probabilistic explanation for the size-effect in crystal plasticity. *Philos. Mag.* **95,** 1829–1844 (2015).
18. Derlet, P. M. & Maass, R. Universal power-law strengthening in metals? *Scripta Mater.* **109,** 19–22 (2015).
19. Csikor, F. F., Motz, C., Weygand, D., Zaiser, M. & Zapperi, S. Dislocation avalanches, strain bursts, and the problem of plastic forming at the micrometer scale. *Science* **318,** 251–254 (2007).
20. El-Awady, J. A. Unravelling the physics of size-dependent dislocation-mediated plasticity. *Nature Communications* **6,** 5926 (2015).
21. Zhou, C., Beyerlein, I. & LeSar, R. Plastic deformation mechanisms of fcc single crystals at small scales. *Acta Mater.* **59,** 7673–7682 (2011).
22. Chen, Lisa Y., He, M.-R., Shin, J., Richter, G. & Gianola, Daniel S. Measuring surface dislocation nucleation in defect-scarce nanostructures. *Nature Mater.* **14,** 707–713 (2015).
23. Li, J. Dislocation nucleation: diffusive origins. *Nature Mater.* **14,** 656–657 (2015).
24. Kampen, N. G. V. *Stochastic processes in Physics and Chemistry* (NorthHolland: Elsevier, 1992).
25. Hussein, Ahmed M., Rao, Satish I., Uchic, Michael D., Dimiduk, Dennis M. & El-Awadya, J. A. Microstructurally based cross-slip mechanisms and their effects on dislocation microstructure evolution in fcc crystals. *Acta Mater.* **85,** 180–190 (2015).
26. Yu, Q., Mishra, R. K., Morris, Jr., J. W. & Minor, A. M. The effect of size on dislocation cell formation and strain hardening in aluminium. *Philos. Mag.* **94,** 2062–2071 (2014).
27. Kocks, U. F., Argon, A. S. & Ashby, M. F. Thermodynamics and kinetics of slip. *Prog. Mater. Sci.* **19,** 291 (1975).
28. Kocks, U. F. & Mecking, H. Physics and phenomenology of strain hardening: the FCC case. *Prog. Mater. Sci.* **48,** 171–273 (2003).
29. Huang, G.-R., Saakian, D. B., Rozanova, O., Yu, J.-L. & Hu, C.-K. Exact solution of master equation with Gaussian and compound Poisson noises. *J. Stat. Mech. Theor. Exp.* **2014,** 11033 (2014).
30. Bei, H., Shim, S., Pharr, G. M. & George, E. P. Effects of pre-strain on the compressive stress-strain response of Mo-alloy single-crystal micropillars. *Acta Mater.* **56,** 4762–4770 (2008).
31. El-Awady, J. A. *et al.* Pre-straining effects on the power-law scaling of size-dependent strengthening in Ni single crystals. *Scripta Mater.* **68,** 207–210 (2013).
32. Hussein, A. M. & El-Awady, J. A. Quantifying dislocation microstructure evolution and cyclic hardening in fatigued face-centered cubic single crystals. *J. Mech. Phys. Solids* **91,** 126–144 (2016).
33. Friedman, N., Cai, L. & Xie, X. S. Linking stochastic dynamics to population distribution: an analytical framework of gene expression. *Phys. Rev. Lett.* **97,** 168302 (2006).
34. Bouchaud, J.-P. & Mezard, M. Universality classes for extreme-value statistics. *J. Phys. A Math. Gen.* **30,** 7997 (1997).
35. Zaiser, M. & Nikitas, N. Slip avalanches in crystal plasticity: scaling of the avalanche cut-off. *J. Stat. Mech. Theor. Exp.* **2007,** 04013 (2007).

36. Rao, S. I. *et al.* Athermal mechanisms of size-dependent crystal flow gleaned from three-dimensional discrete dislocation simulations. *Acta Mater.* **56,** 3245–3259 (2008).
37. Wu, J. H., Tsai, W. Y., Huang, J. C., Hsieh, C. H. & Huang, Guan-Rong. Sample size and orientation effects of single crystal aluminum. *Mater. Sci. Eng. A* **662,** 296–302 (2016).
38. Greer, J. R., Weinberger, Christopher R. & Cai, W. Comparing the strength of fcc and bcc sub-micrometer pillars: Compression experiments and dislocation dynamics simulations. *Mater. Sci. Eng. A* **493,** 21–25 (2008).
39. Buzzi, S., Dietiker, M., Kunze, K., Spolenak, R. & Lffler, J. F. Deformation behavior of silver submicrometer-pillars prepared by nanoimprinting. *Philos. Mag.* **89,** 869–884 (2009).

Acknowledgements

Author Contributions

Guan-Rong Huang constructed the theoretical model, performed analytical calculation, prepared Figures 1 and 2, and wrote the manuscript. J.C. Huang guided the project, provided conceptual advice, and assisted interpretation of results. W.Y. Tsai provided conceptual advice and prepared Figure 3. All authors critically revised and reviewed the manuscript.

Additional Information

Competing financial interests: The authors declare no competing financial interests.

How to cite this article: Huang, G.-R. *et al.* Origin of sample size effect: Stochastic dislocation formation in crystalline metals at small scales. *Sci. Rep.* **6**, 39242; doi: 10.1038/srep39242 (2016).

Publisher's note: Springer Nature remains neutral with regard to jurisdictional claims in published maps and institutional affiliations.